

Robust Detector of Multi-Pixel Targets Using a Sequence of Images

Victor Golikov^{*}, David Kantun Marin, Hussain Alazki

Universidad Autonoma del Carmen, calle 56 esq. av. Concordia, No.4, Facultad de Ingenieria, Ciudad del Carmen, Camp., Mexico. C.P. 24180
Corresponding Author: Victor Golikov

Abstract : We design and assess an algorithm to detect a multi-pixel target of an unknown spatial size, shape and position in a sequence of images in the presence of an additive Gaussian background clutter and a channel noise. The presence of the target decreases the background plus noise power that hence may be different under the null and alternative hypotheses. We use the generalized likelihood ratio (GLR) approach to derive a modified multi-pixel matched subspace detector (MMMSD) that is sensitive to both energy in the target subspace and reduced energy in the orthogonal subspace. The derived algorithm combines the multi-pixel matched subspace detector and multi-pixel background-plus-noise power change detector in a unique scheme. The crucial characteristic of the proposed detector is that prior knowledge of the target size, shape and position is not required. The designed detector is theoretically proved and numerically evaluated. Numerical simulations attest the validity of the theoretical analysis and show that the proposed MMMSD outperforms the known detector in the case of unknown spatial parameters of the target.

Keywords: Multi-pixel subspace detection, sequence of optical digital images, signal-dependent background clutter.

Date of Submission: 11-01-2018

Date of acceptance: 27-01-2018

I. INTRODUCTION

Target detection from optical/infrared images has been considered by many authors [1-25]. A number of approaches has been previously developed for the detection of targets in the presence of the dominant background clutter and noise. The GLR approach is a well known tool among the signal processing community and has been exploited in many detection problems [13], [14]. Reed and Yu [22] considered GLR target detection from a sequence of optical images, which are first preprocessed by removing local means so that the background clutter and noise will approximately have the Gaussian distribution. Distributed target detectors in Gaussian and Compound-Gaussian noise have been developed in [15-19]. In [21, 22, 25], the detector uses one pixel in an image sequence even though the target may occupy more than one pixel. It was shown [21] that the performance of the multi-pixel detector outperforms the performance of the detector using only one pixel. All quoted above detectors exhibit one drawback: they generally fail when the signal-to-background ratio (SBR) is low. The introduction of the paper should explain the nature of the problem, previous work, purpose, and the contribution of the paper. The contents of each section may be provided to understand easily about the paper.

In video/infrared systems, the target may completely cover the pixel cells on the fluctuating surface and, in this case, the received signal contains only target signal plus channel noise. Hence, the presence of the target removes the background clutter from the received signal. In this case, it is more appropriate to use the GLR approach with different background plus noise power under the two hypotheses. Specifically, each pixel contains the background-plus-noise power under the null hypothesis and the signal-plus-noise power under the alternative hypothesis only in the case of the presence of the target in this pixel. A modified GLR approach associated with the hypothesis dependent background clutter power has been recently proposed by us for subpixel optical/infrared objects [24, 25]. In our work, the detection problem of multi-pixel targets is being solved using the GLR approach that processes a certain set of pixels (subimage) in a sequence of images. We find the GLR test (GLRT) for a partially known deterministic multi-pixel target signal by using a set of K subimages of the same scene obtained from sequential observation in time. We extend the GLR approach to a general case when the possible object is contained within unknown N pixels located in the subimage of size L . The object may be partially or completely present within a received $K \times L$ subimage data matrix. Among the L pixels, N ($N \leq L$) pixels are a sum of the deterministic signal and Gaussian channel noise, while the remaining $L - N$ pixels are a sum of a Gaussian background and Gaussian channel noise. The received subimage data matrix is used to estimate the sample background power for each pixel only under the alternative hypothesis. The proposed detector (MMMSD) is sensitive to both the SBR and size of the area unoccupied by the target within

the subimage. We contrast it with the known detector designed for known spatial parameters of the target. The theoretical results and computer simulation show that the detection performance of the proposed detector considerably outperforms that of the known detector.

II. MULTI-PIXEL GLRT FOR RANGE DISTRIBUTED TARGETS

In this section, we derive the GLRT for a multi-pixel range distributed target in the case of unknown a priori size, position and shape of the target. We consider the problem of detecting a multi-pixel optical target in the sequence of K digital images with a random homogeneous Gaussian background and channel noise. We assume that the multi-pixel object of the size N may be present completely or partially anywhere in the subimage of the size L . We assume that the subimage is partially covered by the target, and the presence of the target changes the background-plus-noise power in the pixels covered by the target. Let $l \in \Omega \equiv \{1, \dots, L\}$ be a subset of integers indexing the pixels in the subimage. We assume that the homogeneous background vectors \mathbf{c}_l and channel noise vectors \mathbf{n}_l can be modeled as K -dimensional (for K images) normal random vectors, i.e. $\mathbf{c}_l \sim N(0, \sigma_c^2 \mathbf{I})$ (after preprocessing) and $\mathbf{n}_l \sim N(0, \sigma_n^2 \mathbf{I})$. Moreover, suppose that the \mathbf{c}_l and \mathbf{n}_l are random vectors that are independent from pixel to pixel. Finally, let $\Omega_T \equiv \{1, \dots, N\} \subset \Omega$ ($N \leq L$) be the subset of integers indexing the pixels, which may contain a partially unknown object under the H_1 hypothesis. This partially unknown object is modeled as $\mathbf{s}_i = \mathbf{H}\boldsymbol{\theta}_i$ for $i \in \Omega_T$, where the unknown parameter $\boldsymbol{\theta}_i$ is the amplitude vector that locates the deterministic object signal in the signal subspace spanned by the $p < K$ columns of a known target mode matrix $\mathbf{H} = [\mathbf{h}_1, \dots, \mathbf{h}_p] = \mathbf{C}^{K \times p}$ [13]. \mathbf{H} is the Vandermonde matrix with discrete complex exponential elements (Fourier components). We develop a hypothesis test that distinguishes the signal-plus-noise hypothesis (H_1) from the background-plus-noise hypothesis (H_0). Consider two hypotheses:

$$\begin{cases} H_0: & \mathbf{x}_l = \mathbf{c}_l + \mathbf{n}_l, & l \in \Omega, \\ H_1: & \begin{cases} \mathbf{x}_i = \mathbf{s}_i + \mathbf{n}_i, & i \in \Omega_T, \\ \mathbf{x}_j = \mathbf{c}_j + \mathbf{n}_j, & j \in \Omega \setminus \Omega_T, \end{cases} \end{cases} \quad (1)$$

where $\Omega \setminus \Omega_T \equiv \{N + 1, \dots, L\}$ denotes the difference between subsets Ω and Ω_T . We derive two different GLRTs based on two different hypotheses about the size, shape, and position of a possible object. First, we consider the case when the size, shape, and position of a possible target are a priori known i.e. $\Omega_T = \Omega$. Then, the joint *pdf* under H_1 and H_0 may be written as

$$p_1(\mathbf{x}_1, \dots, \mathbf{x}_L; \boldsymbol{\theta}_i | H_1) = \frac{c}{|\sigma_n^2 \mathbf{I}|^{L/2}} \exp \left\{ -\frac{1}{2} \sum_{i=1}^L (\mathbf{x}_i - \mathbf{s}_i)^T (\sigma_n^2 \mathbf{I})^{-1} (\mathbf{x}_i - \mathbf{s}_i) \right\} \quad (2)$$

$$p_0(\mathbf{x}_1, \dots, \mathbf{x}_L; H_0) = \frac{c}{|\sigma_{c+n}^2 \mathbf{I}|^{N/2}} \exp \left\{ -\frac{1}{2} \sum_{i=1}^L \mathbf{x}_i^T (\sigma_{c+n}^2 \mathbf{I})^{-1} \mathbf{x}_i \right\}, \quad (3)$$

where $|\cdot|$ is the determinant of a matrix, $\sigma_{c+n}^2 = \sigma_c^2 + \sigma_n^2$, and c is the *pdf* normalization constant. According to the Neyman-Pearson criterion, the optimum solution to the problem of testing hypotheses (1) is the likelihood ratio test (for known parameters) [13] or the GLR (for unknown parameters) [9, 12]. In the case of known size, position and shape of the target the GLR statistic can be formulated as

$$\Lambda_{kn} = \frac{\max_{\boldsymbol{\theta}_t} p_1(\mathbf{x}_1, \dots, \mathbf{x}_L; \boldsymbol{\theta}_t | H_1)}{p_0(\mathbf{x}_1, \dots, \mathbf{x}_L; H_0)}. \quad (4)$$

It is well known that the maximum of p_1 with respect to $\boldsymbol{\theta}_t$ is attained by substituting the true parameter $\boldsymbol{\theta}_t$ with the maximum likelihood estimate (MLE) of the $\boldsymbol{\theta}_t$

$$\hat{\boldsymbol{\theta}}_t = (\mathbf{H}^H \mathbf{H})^{-1} \mathbf{H}^H \mathbf{x}_t. \quad (5)$$

Then, using some algebra, the known GLRT-based detector named T_{kn} is given by the following statistical test

$$T_{kn} = \sum_{i=1}^N \left\{ \frac{1}{\sigma_{c+n}^2} \mathbf{x}_i^T \mathbf{P}_s \mathbf{x}_i - q \mathbf{x}_i^T \mathbf{P}_s^\perp \mathbf{x}_i \right\} \underset{< H_0}{\overset{> H_1}{>}} \eta, \quad (6)$$

where $q = \sigma_n^{-2} - \sigma_{c+n}^{-2}$, \mathbf{P}_s is $K \times K$ orthogonal projection matrix onto the signal subspace, $\mathbf{P}_s^\perp = \mathbf{I} - \mathbf{P}_s$ is $K \times K$ orthogonal projection matrix onto the subspace orthogonal to the signal subspace $\langle H \rangle$, \mathbf{I} is $K \times K$ unit matrix, and η is a threshold.

Secondly, we consider the case when the size, shape, and position of a possible target are a priori unknown. We introduce the unknown parameter Ω_T , that denotes the subset of integers indexing the pixels, unknown background plus noise variance $\sigma_{1,i}^2$ for each pixel-vector under hypothesis H_1 and unknown target abundance vector $\boldsymbol{\theta}_i$. The GLR is formulated as

$$\Lambda_{um} = \frac{\max_{\theta_i, \Omega_T, \sigma_{1,i}^2} p_1(\mathbf{x}_1, \dots, \mathbf{x}_L; \sigma_{1,i}^2, \Omega_T, \theta_i | H_1)}{p_0(\mathbf{x}_1, \dots, \mathbf{x}_L; | H_0)}, \quad (7)$$

where the numerator is maximized by independent varying $\sigma_{1,i}^2$, θ_i and Ω_T . The MLE of the $\sigma_{1,i}^2$ has two solutions:

$$\hat{\sigma}_{1,i}^2 = \frac{\mathbf{x}_i^T \mathbf{P}_S^\perp \mathbf{x}_i}{K-p} \text{ and } \hat{\sigma}_{1,i}^2 = \frac{\mathbf{x}_i^T \mathbf{x}_i}{K}, \quad (8)$$

where p is the rank of the target subspace $\langle H \rangle$. Previous assumptions for the homogeneous background with known variance σ_{c+n}^2 under null hypothesis and unknown $\hat{\sigma}_{1,i}^2$ under alternative hypothesis imply that the joint pdf under H_1 and H_0 may be written as

$$p_1(\mathbf{x}_1, \dots, \mathbf{x}_L; \Omega_T, \hat{\sigma}_{1,i}^2, \hat{\theta}_t | H_1) = \frac{c}{\left(\prod_{i=1}^L |\hat{\sigma}_{1,i}^2 \mathbf{I}|\right)^{1/2}} \prod_{i \in \Omega_T} \exp\left[-\frac{1}{2}(\mathbf{x}_i - \mathbf{s}_i)^T (\hat{\sigma}_{1,i}^2 \mathbf{I})^{-1} (\mathbf{x}_i - \mathbf{s}_i)\right] \times \prod_{j \in \Omega \setminus \Omega_T} \exp\left[-\frac{1}{2} \mathbf{x}_j^T (\hat{\sigma}_{1,j}^2 \mathbf{I})^{-1} \mathbf{x}_j\right], \quad (9)$$

$$p_0(\mathbf{x}_1, \dots, \mathbf{x}_L; | H_0) = \frac{c}{|\sigma_{c+n}^2 \mathbf{I}|^{L/2}} \exp\left\{-\frac{1}{2} \sum_{l=1}^L \mathbf{x}_l^T (\sigma_{c+n}^2 \mathbf{I})^{-1} \mathbf{x}_l\right\}. \quad (10)$$

Substitutions θ_i (5) and $\hat{\sigma}_{1,i}^2$ (8) into the p_1 (7) yield

$$\Lambda_{um} = \max_{\Omega_T} \frac{(\sigma_{c+n}^2)^{KL/2} \exp\left[\sum_{i=1}^L \left(\frac{\mathbf{x}_i^T \mathbf{x}_i}{2\sigma_{c+n}^2}\right) - \sum_{j=1}^N \left(\frac{(K-p)\mathbf{x}_j^T \mathbf{P}_S^\perp \mathbf{x}_j}{2\mathbf{x}_j^T \mathbf{P}_S^\perp \mathbf{x}_j}\right) - \sum_{j=N+1}^L \left(\frac{(K-p)\mathbf{x}_j^T \mathbf{x}_j}{2\mathbf{x}_j^T \mathbf{P}_S^\perp \mathbf{x}_j}\right)\right]}{\left(\prod_{i=1}^L \frac{\mathbf{x}_i^T \mathbf{P}_S^\perp \mathbf{x}_i}{K-p}\right)^{K/2}} \\ = \max_{\Omega_T} \frac{(\sigma_{c+n}^2)^{KL/2} \exp\left[\sum_{i=1}^L \left(\frac{\mathbf{x}_i^T \mathbf{x}_i}{2\sigma_{c+n}^2}\right) - \frac{LK-pN}{2}\right]}{\left(\prod_{i=1}^L \frac{\mathbf{x}_i^T \mathbf{P}_S^\perp \mathbf{x}_i}{K-p}\right)^{K/2}}. \quad (11)$$

Further, we use a straightforward maximization in (11). Since $LK > pN$, it follows immediately that the maximum of Λ_{um} with respect to Ω_T (or N) is obtained by replacing the unknown parameter N by known L . Taking the logarithm of the $K/2$ -th root of Λ_{um} , the proposed GLRT-based detector named MMMSD is given by the following statistical test:

$$T_{um} = \sum_{i=1}^L \left(\frac{\mathbf{x}_i^T \mathbf{x}_i}{K\sigma_{c+n}^2} - \frac{K-p}{K} - \ln \frac{\mathbf{x}_i^T \mathbf{P}_S^\perp \mathbf{x}_i}{(K-p)\sigma_{c+n}^2} \right). \quad (12)$$

We can rewrite the proposed statistical test in the following form

$$T_{um} = \sum_{i=1}^L \left(\frac{\mathbf{x}_i^T \mathbf{P}_S \mathbf{x}_i}{K\sigma_{c+n}^2} - \frac{K-p}{K} \frac{\mathbf{x}_i^T \mathbf{P}_S^\perp \mathbf{x}_i}{(K-p)\sigma_{c+n}^2} - \frac{K-p}{K} - \ln \frac{\mathbf{x}_i^T \mathbf{P}_S^\perp \mathbf{x}_i}{(K-p)\sigma_{c+n}^2} \right). \quad (13)$$

Next we assume that $p \ll K$ and statistical test T_{um} can be rewritten as

$$T_{um} \approx \sum_{i=1}^L \left(\frac{\mathbf{x}_i^T \mathbf{P}_S \mathbf{x}_i}{K\sigma_{c+n}^2} + \frac{\mathbf{x}_i^T \mathbf{P}_S^\perp \mathbf{x}_i}{(K-p)\sigma_{c+n}^2} - \ln \frac{\mathbf{x}_i^T \mathbf{P}_S^\perp \mathbf{x}_i}{(K-p)\sigma_{c+n}^2} - 1 \right) = \sum_{i=1}^L \left(\frac{\mathbf{x}_i^T \mathbf{P}_S \mathbf{x}_i}{K\sigma_{c+n}^2} + A(\mathbf{x}_i) \right), \quad (14)$$

$$\text{where } A(\mathbf{x}_i) \approx \frac{1}{2} \left(\frac{\hat{\sigma}_{1,i}^2}{\sigma_{c+n}^2} - 1 \right)^2. \quad (15)$$

We observe that T_{um} and T_{kn} (14 and 6) differ in the way they remove the power in the subspace orthogonal to signal subspace $\langle H \rangle$ from the total power. The first terms in both algorithms (T_{um} and T_{kn}) are the same (matched subspace detector (MSD)) but the second terms are different. The value of the second term for each pixel occupied by target depends on hypotheses H_0 and H_1 . The impact of the second term on the detection performance depends on ratio between their values under H_0 and H_1 . One can see that $A(\mathbf{x}_i) \gg \frac{\mathbf{x}_i^T \mathbf{P}_S^\perp \mathbf{x}_i}{K\sigma_{c+n}^2}$ especially in case of a small noise-to-background-plus-noise ratio $d = \frac{\sigma_n^2}{\sigma_{c+n}^2}$. Since the real target size, position and shape are rarely exactly known in practice, it is interesting to consider the performance of the proposed statistical test T_{um} and compare it to known statistical test T_{kn} .

III. DETECTION PERFORMANCE ANALYSIS

In this section, we derive the asymptotic distributions of the test T_{um} under the both hypotheses with a view to evaluate the detection performance of the test in terms of probability of detection. Since \mathbf{x}_i is drawn from a multivariate Gaussian distribution, with zero mean and covariance matrices $\sigma_{c+n}^2 \mathbf{I}$ and $\sigma_n^2 \mathbf{I}$, it follows that [13]

$$T_{MSD} = \sum_{i=1}^L \frac{\mathbf{x}_i^T \mathbf{P}_s \mathbf{x}_i}{K \sigma_c^2} \sim \begin{cases} \frac{1}{K} \chi_{Lp}^2(0) & \text{under } H_0 \\ \frac{1}{K} \chi_{(L-N)p}^2(0) & \text{for } i \in \Omega \setminus \Omega_T \\ \frac{d}{K} \chi_{Np}^2(\lambda) & \text{for } i \in \Omega_T \end{cases} \quad \text{under } H_1 \quad (16)$$

where sign \sim means distributed as, non-centrality parameter $\lambda = \frac{Ns^T s}{\sigma_n^2}$. Further we obtain

$$\sum_{i=1}^L \frac{\mathbf{x}_i^T \mathbf{P}_s^\perp \mathbf{x}_i}{(K-p)\sigma_c^2} \sim \begin{cases} \frac{1}{K-p} \chi_{L(K-p)}^2(0) & \text{under } H_0 \\ \frac{1}{K-p} \chi_{(L-N)(K-p)}^2(0) & \text{for } i \in \Omega \setminus \Omega_T \\ \frac{d}{K-p} \chi_{N(K-p)}^2(0) & \text{for } i \in \Omega_T \end{cases} \quad \text{under } H_1 \quad (17)$$

In order to come up with manageable expressions, we investigate an asymptotic approach, assuming that the number of images K is large. As K grows large, it is well known that the chi-square distribution $\chi_K^2(0)$ converges to a Gaussian distribution with the mean K and variance $2K$. It follows that

$$\frac{\mathbf{x}_i^T \mathbf{P}_s^\perp \mathbf{x}_i}{(K-p)\sigma_c^2} \rightsquigarrow \begin{cases} N\left(1, \frac{2}{K-p}\right) & \text{under } H_0 \\ N\left(1, \frac{2}{K-p}\right) & \text{for } i \in \Omega \setminus \Omega_T \\ N\left(d, \frac{2d^2}{K-p}\right) & \text{for } i \in \Omega_T \end{cases} \quad \text{under } H_1 \quad (18)$$

where \rightsquigarrow means asymptotically distributed. Then, the asymptotic distribution of $\sum_{i=1}^L A(\mathbf{x}_i)$ is given by

$$\sum_{i=1}^L A(\mathbf{x}_i) \rightsquigarrow \begin{cases} \frac{1}{K-p} \chi_L^2(0) & \text{under } H_0 \\ \frac{1}{K-p} \chi_{L-N}^2(0) & \text{for } i \in \Omega \setminus \Omega_T \\ \frac{d^2}{K-p} \chi_N^2\left(\frac{K-p}{2d^2}(1-d)^2 N\right) & \text{for } i \in \Omega_T \end{cases} \quad \text{under } H_1 \quad (19)$$

Therefore, the asymptotic distribution of T_{un} is given by

$$T_{un} \rightsquigarrow \begin{cases} \frac{1}{K} \chi_{Lp}^2(0) + \frac{1}{K-p} \chi_L^2(0) & \text{under } H_0 \\ \frac{d}{K} \chi_{Np}^2(\lambda) + \frac{d^2}{K-p} \chi_N^2\left(\frac{K-p}{2d^2}(1-d)^2 N\right) + \frac{1}{K} \chi_{(L-N)p}^2(0) + \frac{1}{K-p} \chi_{L-N}^2(0) & \text{under } H_1 \end{cases} \quad (20)$$

In order to come up with exploitable expressions, we examine a further approximation to (20)

$$T_{un} \rightsquigarrow \begin{cases} \frac{1}{K} \chi_{L(p+1)}^2(0) & \text{under } H_0 \\ \frac{d}{K} \chi_{L(p+1)}^2(\lambda + \lambda_1) & \text{under } H_1 \end{cases}, \quad (21)$$

where $\lambda_1 = \frac{(K-p)(d-1)^2 N}{2d^2}$. The above expression holds for large K and $d \approx 1$. The distribution derived above enable one to obtain the receivers operating characteristics (ROC), that is the probability of detection as a function of the probability of false alarm.

IV. NUMERICAL ILLUSTRATIONS

The aim of this section is twofold. On the one hand, through extensive Monte Carlo simulations, we can check that the *pdf* of (18) matches the exact *pdf* of T_{un} . On the other hand, we assess the performance of the statistics T_{un} both in terms of false alarm probability (P_{fa}) and detection probability (P_d). We also compare the performance of the proposed T_{un} with the known statistics T_{kn} . Since closed-form expressions for P_{fa} and P_d are not available for the T_{kn} and T_{un} for different parameters variations, we evaluate P_d at fixed P_{fa} using standard Monte Carlo counting techniques based on $100/P_{fa}$ and $100/P_d$ independent trials, respectively. At the analysis stage, one must specify the background and target models. The signal model $s_i = \mathbf{H}\theta_i$ is based on an assumption that we have no prior knowledge about the distribution of θ_i . Therefore, we model θ_i as a deterministic unknown vector. Commonly, the vectors θ_i , $i=1, \dots, N$, are modeled as vectors drawn from a uniformly distributed uncorrelated random sequence. A model of the target mode matrix is a Vandermonde matrix with discrete complex exponential elements

$$H = \begin{bmatrix} 1 & 1 & \dots & 1 \\ h_1 & h_2 & \dots & h_p \\ \vdots & \vdots & \vdots & \vdots \\ h_1^{K-1} & h_2^{K-1} & \dots & h_p^{K-1} \end{bmatrix}, \quad (22)$$

where $h_i = \exp(j2\pi i/K)$, $i \in (0, p)$, $j = \sqrt{-1}$. In order to limit the computational burden, the false alarm probability is chosen as 10^{-3} . Fig.1 illustrates the relation between the detection probability of the MMMSD (T_{un}) and signal-to-noise ratio in each pixel for the different target fill factors (FF=N/L) defined as the percentage of a pixel area occupied by the object. We can compare (see Fig.1) the theoretical performance with simulation results. We can notice that the theoretical expression (18) gives a relatively precise approximation of the real test performance. Fig.2 shows the obtained theoretical receiver operating characteristics (the detection vs false alarm probabilities) for the different FF using the approximation (21) to the asymptotic distribution of T_{un} (20). As we see in Figs. 1,2, the detector performance depends on FF. One can see that for $FF \approx 1$ the performance of the MMMSD is better. In Fig.3, we can compare the performance of the proposed test statistics (12) and known (6). The statistical test (6) is obtained using GLRT for known position, shape and size of target (the target completely occupies the subimage) but the statistical test (12) for unknown position, shape and size of target. An intuitive and qualitative analysis of the difference between T_{un} and T_{kn} allows to conclude that for the $FF \approx 1$ the T_{kn} must be better but in the case of $FF < 1$ the T_{un} must be better.

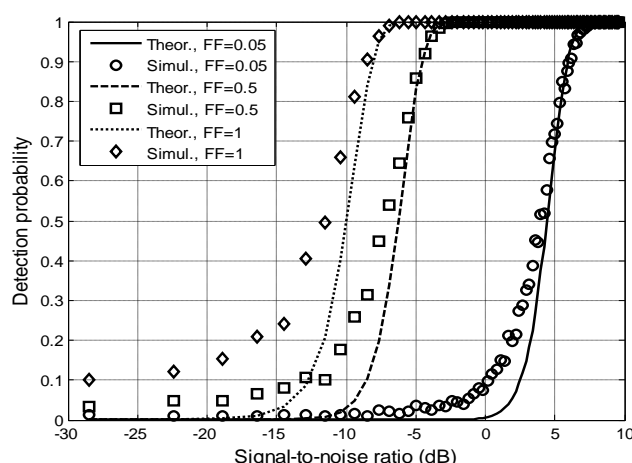


Fig.1. Detection probability vs SNR for different FF, background-to-noise ratio BNR=1.2, $L=20$, $K=20$, $p=4$, $P_{fa}=10^{-3}$ (Theoretical and simulation results for the MMMSD).

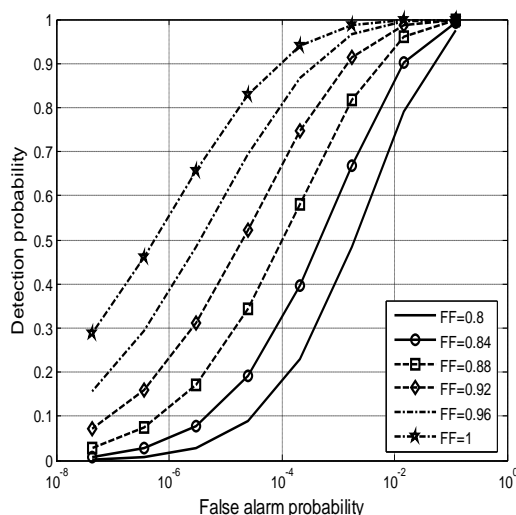


Fig.2. Detection probability vs false alarm probability (ROC) for different FF, $L=50$, $K=20$, $p=4$, BNR=2, SNR=2 (Theoretical results for the MMMSD, see (21)).

One can see in Fig.3 that the quantitative analysis confirms the qualitative one: in the case of $FF < 0.8$ the performance of the T_{un} outperforms the performance of the T_{kn} .

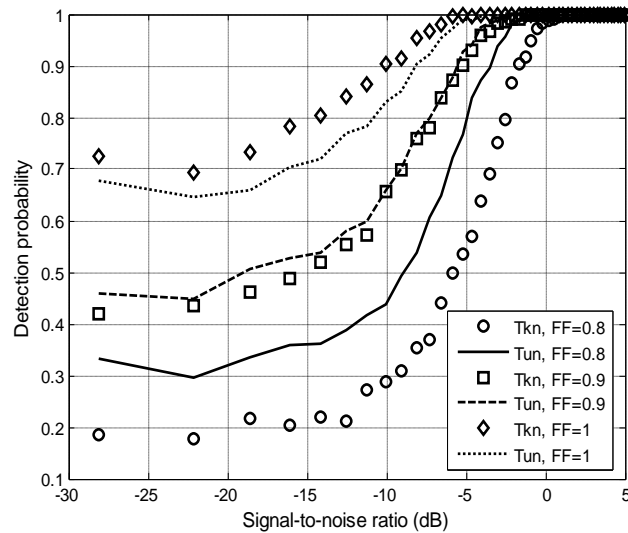


Fig.3. Detection probability vs SNR for different FF, $L=10, K=10, p=2, P_{fa}=10^{-3}$ (Simulation results for T_{un} and T_{kn}).

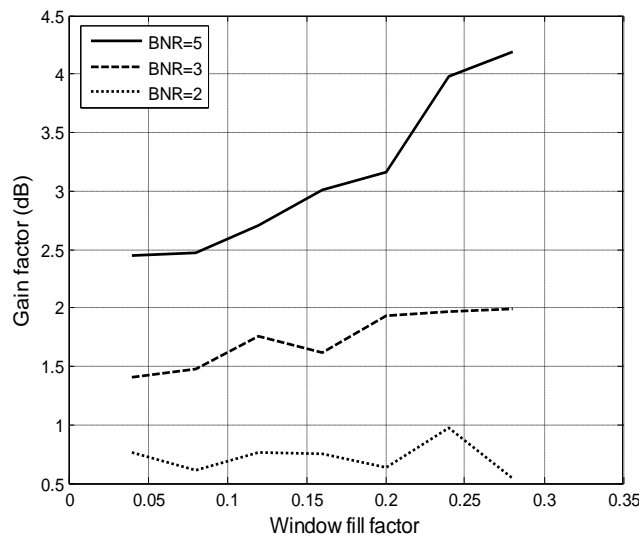


Fig.4. Gain factor vs fill factor for different background-to-noise ratio ($BNR=1/d$), $L=25, K=6, p=2, P_{fa}=10^{-3}$ (Simulation results for T_{un} and T_{kn}).

These results of the comparison (T_{un} and T_{kn}) for the small FF and different signal-to-noise ratio (BNR) are presented in Fig.4. In this figure we use an important parameter of the detector performance: detector gain factor. This factor is defined as the horizontal displacement (at detection probability $P_D=0.8$) between dependences of P_D versus SNR for the T_{un} and T_{kn} (see Fig.3 for example) [24]. One can see that gain factor depends on BNR and can achieve 4 dB. Therefore, the performance of the T_{un} outperforms the performance of the T_{kn} in the case of unknown shape, size and position of the target within the subimage. Moreover, its performance is robust with respect to the shape and position of the target within the subimage.

II. CONCLUSION

In contrast to traditional methods, we derive the GLRT using the background power estimation only under the alternative hypothesis. This is an interesting novel twist on the usual approach to unstructured multi-pixel detection. This approach extends well-known existing ones on matched subspace detection in the hypothesis dependent multi-pixel model that we consider. The structure of the proposed MMMSD differs from the known detector by adding the term proportional to the sum of the logarithms of the ratios between the background variances under H_1 and H_0 . The numerical simulations confirm the validity of the theoretical

analysis and show that the novel detector outperforms the classical one considerably. The crucial characteristic of the proposed detector is that prior knowledge of the target shape and position is not required, and its performance is robust with respect to the shape and position of the target.

REFERENCES

- [1]. C.D. Wang, Adaptive spatial/temporal/spectral filters for background clutter suppression and target detection, *Optical Engineering*, 21(12),1982, 1033-1038.
- [2]. A. Borghgraef, O. Barnich, F. Lapiere, M. Van Droogenbroeck, W. Philips, and M. Achery, An Evaluation of Pixel-Based Methods for the Detection of Floating Objects on the Sea Surface, *EURASIP Journal on Advances in Signal Processing*, 2010, art. ID 978451.
- [3]. E. Jeff Holder, Orthogonal Space Projection (OSP) Processing for Adaptive Interference Cancellation, *IEEE Signal Processing Letters*, 21(8), 2014. 980-984.
- [4]. T. M. Tu, C. H. Chen, and C. I. Chang, A Noise Subspace Projection Approach to Target Signature Detection and Extraction in an Unknown Background for Hyperspectral Images, *IEEE Trans. Geosci. Remote Sensing*, 36(1),1998, 171-181.
- [5]. Jun Tang, NingLi, Yong Wu, and YingningPeng, On Detection Performance of MIMO Radar: A Relative Entropy-Based Study, *IEEE Signal Processing Letters*, 16 (3),2009, 184-187.
- [6]. S. D. Blostein and T. S. Huang, Detecting Small, Moving Objects in Image Sequences using Sequential Hypothesis Testing, *IEEE Trans. Signal Process.*,39(7), 1991, 1611-1628.
- [7]. Zhihu Wang, Kai Liao, JiulongXiong, and Qi Zhang, Moving Object Detection Based on Temporal Information, *IEEE Signal Processing Letters*, 21(11), 2014, 1403-1408.
- [8]. M. Bruno and J. M. Moura, Multiframe Detector/Tracker: Optimal Performance, *IEEE Trans. Aerosp. Electron. Syst.*, AES-37(3), 2001, 925-944.
- [9]. J. Kelly, An adaptive detection algorithm, *IEEE Trans. Aerosp. Electron. Syst.*, AES-22(2), 1986, 115-127.
- [10]. F. C. Robey, D. L. Fuhrman, E. J. Kelly, and R. Nitzberg, A CFAR adaptive matched filter detector, *IEEE Trans. Aerosp. Electron. Syst.*, 29(1),1992, 208-216.
- [11]. E. Conte, M. Lops, and G. Ricci, Adaptive matched filter detection in spherically invariant noise, *IEEE Signal Processing Letters*, 3(8), 1996, 248-250.
- [12]. S. Kraut, L.L. Scharf, and L.T. McWhorter, Adaptive subspace detectors, *IEEE Transactions on Signal Processing*, 49(1), 2001, 1-16.
- [13]. L. Scharf, *Statistical signal processing: detection, estimation and time series analysis* (Reading, MA: Addison-Wesley, 1991).
- [14]. A. Aubry, A. De Maio, D. Orlando, and M. Piezzo, Adaptive Detection of Point-Like Targets in the Presence of Homogeneous Clutter and Subspace Interference, *IEEE Signal Processing Letters*, 21(7), 2014, 848-853.
- [15]. K. Gerlach, and M.J. Steiner, Adaptive Detection of Range Distributed Targets, *IEEE Transactions on Signal Processing*, 47(7), 1999, 1844-1851.
- [16]. N. Bon, A. Khenchaf, and R. Garello, GLRT Subspace Detection for Range and Doppler Distributed Targets, *IEEE Trans. Aerosp. Electron. Syst.*, 44(2), 2008, 678-694.
- [17]. E. Conte, A. De Maio, and G. Ricci, GLRT-Based Adaptive Detection Algorithms for Range-Spread Targets, *IEEE Trans. Signal Process.*, 49(7), 2001, 1336-1348.
- [18]. F. Bandiera, D. Orlando, and G. Ricci, CFAR Detection of Extended and Multiple Point-Like Targets Without Assignment of Secondary Data, *IEEE Signal Processing Letters*, 13(4), 2006, 240-243.
- [19]. F. Bandiera, O. Besson, and G. Ricci, Adaptive Detection of Distributed Targets in Compound-Gaussian Noise Without Secondary Data: A Bayesian Approach, *IEEE Trans. Signal Process.*, 59(12), 2011, 5698-5708.
- [20]. A. Margalit, I.S. Reed, and R.M. Galgiardi, Adaptive Optical Target Detection Using Correlated Images, *IEEE Trans. Aerosp. Electron. Syst.*, AES-21(5), 1985, 234-246.
- [21]. J. Chen, and I. Reed, A Detection Algorithm for Optical Targets in Clutter, *IEEE Trans. Aerosp. Electron. Syst.*, AES-23(1), 1987, 46-59.
- [22]. I.S. Reed, and Xiaoli Yu, Adaptive Multiple-Band CFAR Detection of an Optical Pattern with Unknown Spectral Distribution, *IEEE Trans. on Acoustics, Speech and Signal Processing*, 38(10), 1990, 548-259.
- [23]. D. Manolakis, Taxonomy of detection algorithms for hyperspectral imaging applications, *Optical Engineering*, 44(6), 2005, 066403.
- [24]. V. Golikov and O. Lebedeva, Adaptive Detection of Subpixel Targets With Hypothesis Dependent Background Power, *IEEE Signal Processing Letters*, 20(8), 2013, 751-754.
- [25]. Bo Du, Yuxiang Zhang, Liangpei Zhang, and Lefei Zhang, A hypothesis independent subpixel target detector for hyperspectral images, *Signal Processing*, 2014, <http://dx.doi.org/10.1016/j.sigpro.2014.08.018>.

Victor Golikov. "Robust Detector of Multi-Pixel Targets Using a Sequence of Images." *IOSR Journal of Engineering (IOSRJEN)*, vol. 8, no. 1, 2018, pp. 07-13.